Feasibility Study of Air-Breathing Turboengines for Horizontal Takeoff and Landing Space Planes

M. Minoda* and K. Sakata†
National Aerospace Laboratory, Chofu, Tokyo 182, Japan
and
T. Tamaki,‡ T. Saitoh,§ and A. Yasuda¶
Ishikawajima-Harima Heavy Industries, Ltd., Tanashi, Tokyo 188, Japan

One of the most challenging key technologies for realizing horizontal takeoff and landing space planes is the development of a propulsion system with which the vehicle can lift some payload to the orbit. In order to reduce the propellant consumption, which is one of the most important requirements for the future powerplant, some kinds of air-breathing engines with attractive features are considered herein. This study focuses on turboengines that are based on the turbomachinery technology, i.e., turbojet with and without afterburner, turboramjet, and some kinds of air-turboramjet engines. The study also focuses on clarifying their performances and mission capabilities for single-stage-to-orbit vehicles. In the performance study, thrust and specific fuel consumption are calculated by off-design analysis. Next, the mission capability for single- and two-stage-to-orbit vehicles is examined in terms of a ratio of an effective remaining weight to takeoff gross weight by the two-dimensional flight analysis. (Effective remaining weight refers to the remaining weight on the final orbit, except the propulsion system weight; in other words, the total of vehicle structure weight and payload of the vehicle.)

Nomenclature

D = drag force
F = gross thrust
Isp^* = mean specific impulse along the flight path
m = vehicle mass
T^* = mean thrust along the flight path
V = flight speed
W_{pay} = payload weight
W_{str} = mean structural weight
W_{to} = takeoff gross weight

I. Introduction

As human activities in space extend in the future, more economic and reliable space transportation systems will be required. The leading countries in the aerospace technology, such as the United States, European countries, and Japan, have already begun to promote their own research programs of future space vehicles that could offer the advantage of full system reusability, aircraft-like operation (horizontal takeoff and landing), safer abort procedures and improved ascent performance. Because of utilization not only for aircraft but also for rocket technology, these vehicles are called space planes.

From the viewpoint of propellant consumption reduction, which is one of the most important requirements for space planes, air-breathing engines are preferably adopted because they utilize oxygen in the atmosphere and consume less oxidizer aboard. Most of the studies recently published for spaceplane propulsion deal with as high a Mach number as possible from takeoff.

Presented as Paper 89-2296 at the AIAA/ASME/SAE/ASEE 25th Joint Propulsion Conference, Monterey, CA, July 10-12, 1989; received July 28, 1989; revision received March 14, 1990. Copyright © 1989 by the American Institute of Aeronautics and Astronautics, Inc. All rights reserved.

*Director, Thermofluid Dynamics Division. Member AIAA.
†Head, Engine Aerodynamics Laboratory. Member AIAA.
‡Manager, Engine Performance Engineering Division. Member AIAA.
§Lead Engineer.
¶Engineer.

The study presented herein, based on our previous study[1,2] that clarified the required performance of air-breathing engines, especially of turboengines for a single-stage-to-orbit (SSTO) vehicle, concerns the performance analysis of turboengines, including turboramjet (TRJ), pure turbojet (TJ), gas generator cycle air-turboramjet (GG-ATR), expander cycle ATR (Exp-ATR), and part-expander cycle ATR (PE-ATR). Here, PE-ATR is defined as a kind of GG-ATR that has a heat exchanger with high efficiency around the exhaust system (combustor and nozzle). The hydrogen fuel is preheated partly before going to the gas generator, but the heat absorption is restricted to that available in a cooling jacket surrounding the combustor nozzle.

Two-stage-to-orbit (TSTO) vehicles are said to have advantages over SSTO vehicles: less advanced technology required and lower development risk. Today, TSTO missions are studied in many countries, especially in Europe.[3,4] The SAENGER transportation concept proposed by Messerschmitt-Boelkow-Blohm (MBB) in Germany[5] is one of the most famous TSTO mission concepts, which consists of a first stage equipped with turboramjet engines and a rocket-powered second stage.

This study consists of the performance study analysis of the promising turboengine systems described earlier and the flight analysis of the space plane that is propelled by them. Thrust and specific impulse *Isp* of each engine system are calculated and compared. The influence of the design pressure ratio and turbine inlet temperature (TIT) is also examined. Next, the SSTO flight analysis enables evaluation of the engine capability, which is measured by the ratio of the remaining weight on the final orbit to the takeoff gross weight. (Remaining weight does not include engine weight: it consists of the structural weight of the vehicle and the payload weight.) The feasibility of a TSTO vehicle is also obtained by the flight analysis and is compared with that of a SSTO vehicle.

II. Air-Breathing Propulsion Systems

A wide variety of possible air-breathing engines to propel SSTO and TSTO vehicles have been studied. Among them, this study focuses on turboengines, including the TJ engine, the TRJ engine, and the ATR engine.

Figures 1a and 1b illustrate the TJ without and with an afterburner, respectively. The former is referred to as a dry

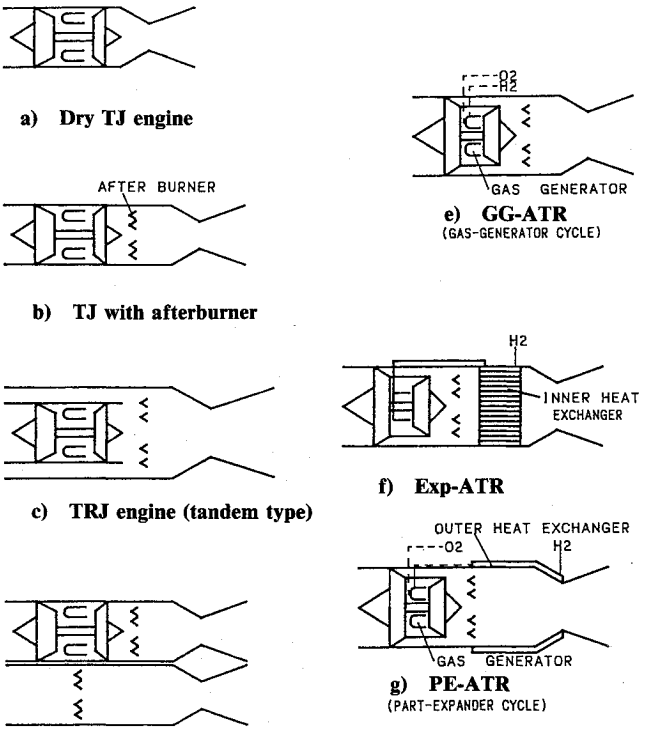

Fig. 1 Conceptual schematics of turboengine systems.

TJ, hereafter. The primary advantage of a TJ engine is its largely conventional design. The fact that is has propelled a great many airplanes for more than 40 years reduces the risks that the other new-concept engines are associated with. Its maximum operational speed is generally lower than TRJ and ATR engines, etc., due to the limit of heat resistance of the compressor.

Figures 1c and 1d show the schematics of the tandem-type and the over/under-type TRJ engine, respectively. The TRJ engine is the directly combined engine of the TJ engine, which operates from takeoff to about Mach 3, and the RJ engine, which extends the flight range up to about Mach 7. It can keep a higher *Isp* in the wide Mach range, but has the disadvantage of the complexity of engine operation, especially in the transient mode between TJ and RJ. The tandem-type TRJ engine, in which the reheat and nozzle systems are common to both the TJ and RJ engines, is lighter than the over/under type, but it needs a more complex operation-control system because of the mixing of two different flows in the ram combustion chamber.

The ATR engine is also one of the most preferrable propulsion systems for the space plane. Its cycle is characterized by using a propellant (hydrogen) as the working fluid in the turbine that provides power to the fan. The three types of ATR engines that are considered in the present study, GG-ATR, Exp-ATR, and PE-ATR, are shown in Figs. 1e–1g, respectively. The GG-ATR engine is equipped with a gas generator that generates fuel rich combustion gas using fuel and oxygen. Since the GG-ATR engine needs an oxidizer besides fuel, its *Isp* is lower than the Exp-ATR's. Its total engine system is so simple that its weight is lighter than the TRJ and Exp-ATR engines. In the Exp-ATR system, the turbine is driven by fuel heated in the heat exchanger located in the combustion gas flow. Therefore, no oxidizer is required, which causes its high *Isp*. The ATR engine with a heat exchanger only around the exhaust system (i.e., with no heat exchanger in the combustion chamber), which is named the PE-ATR engine, represents an intermediate between the previous two types of ATR engines. In this system, hydrogen gas is heated up to 500–900 K by the outer heat exchanger before it burns in the gas generator, so

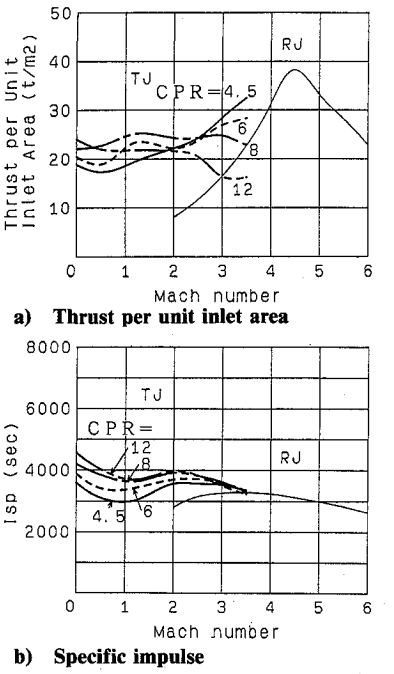

Fig. 2 Performance of TRJ (TIT = 1500°C): dynamic pressure on the flight path is 80 kPa.

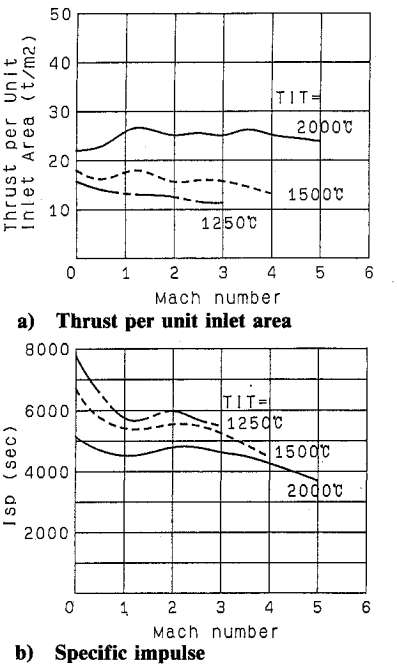

Fig. 3 Performance of dry TJ: design pressure ratio (sea-level static) is 6.0.

that less oxidizer is needed than in the GG-ATR engine. No inner heat exchanger causes the reduction of the weight of the engine system.

III. Engine Performance Analysis

This section shows the result of the off-design (from takeoff to M6) performance analysis conducted for the turboengines mentioned in the previous section. The dynamic pressure on the operating points is assumed to be 80 kPa for all cases.

Figures 2 show the net thrust per unit inlet area and specific impulse of the TRJ engine. The inlet area is defined by the compressor inlet area in the case of the TJ engine and by the cross section of the combustion chamber in the RJ engine. The equivalence ratio of 1 (stoichiometric) in the reheat and the ram combustion chamber is assumed, and TIT is held to be

1500°C constant throughout the operation. Each of four lines in the figure corresponds to the design (sea-level static) compressor pressure ratio (CPR) of 4.5, 6.0, 8.0, 12.0, respectively. The figure indicates that the lower CPR gives the higher thrust in the high flight speed. However, the TJ with CPR = 8.0 gives the highest thrust at the transonic speed, which is one of the critical points that determines the thrust size. The thrust of the RJ is decreasing above the Mach 5.0 because of the limitation of the maximum intake area. The *Isp* of the RJ engine becomes higher than those of the TJ engines above Mach 3.5, which is considered to be the switching point of the TJ and RJ engines in order to keep higher *Isp*.

The influence of TIT on the performance of the TJ engine without A/B, i.e., dry TJ, is shown in Figs. 3, in which the design pressure ratios are held to be 6.0 constant. It points out that dry TJ with TIT = 2000°C can generate the thrust up to Mach 5, namely, the direct transient from dry TJ to the scramjet may be possible without the subsonic ramjet in the SSTO mission. This combined system contributes the considerable weight reduction of the propulsion system, but high heat resistance is needed for both the compressor and the turbine of the TJ engine. On the other hand, Figs. 4 show no drastic influence of TIT on the performance of the TJ engine with afterburning because the stoichiometric combustion assumed in the reheat section compensates for the difference of equivalence ratio in the main combustor.

Figures 5 show the performance of the dry TJ with TIT = 2000°C, in which the design pressure ratio is varied from 4.5 to 12.0. It is shown that the lower CPR gives the higher thrust at high Mach number. The lower CPR also con-

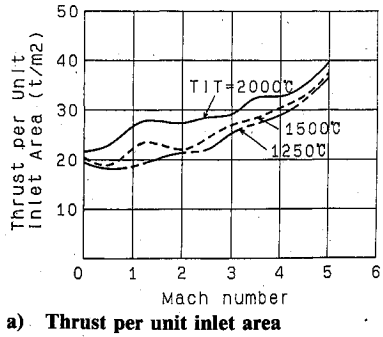

a) Thrust per unit inlet area

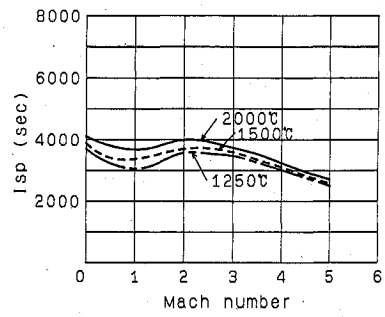

b) Specific impulse

Fig. 4 Performance of TJ with afterburner: design pressure ratio (sea-level static) is 6.0.

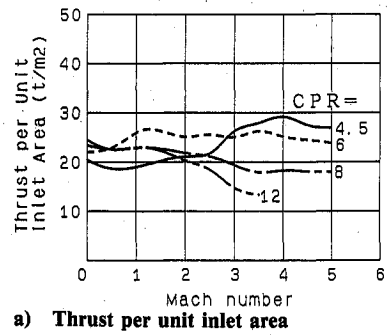

a) Thrust per unit inlet area

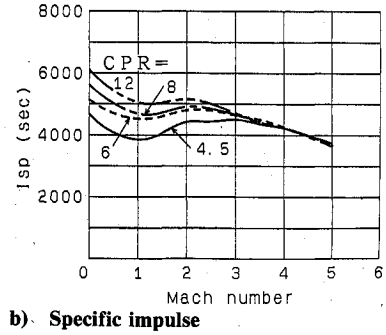

b) Specific impulse

Fig. 5 Performance of dry TJ (TIT = 2000°C).

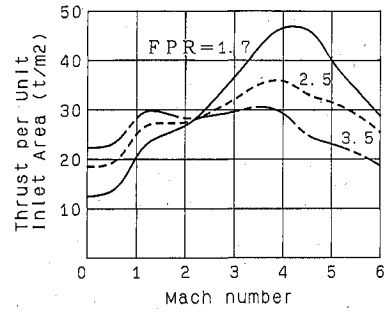

a) Thrust per unit inlet area

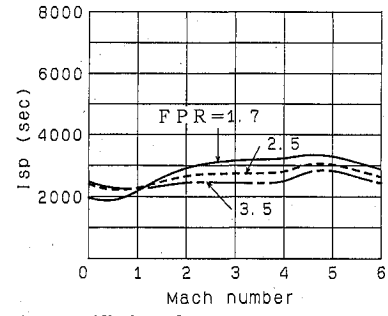

b) Specific impulse

Fig. 6 Performance of GG-ATR.

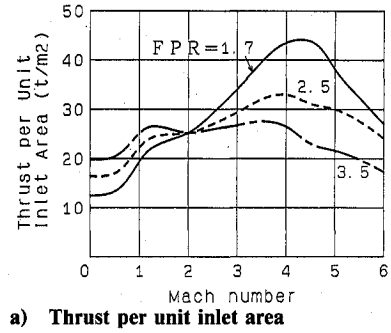

a) Thrust per unit inlet area

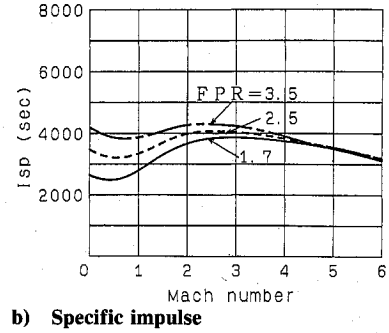

b) Specific impulse

Fig. 7 Performance of Exp-ATR.

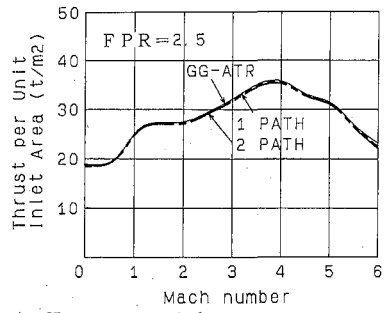

a) Thrust per unit inlet area

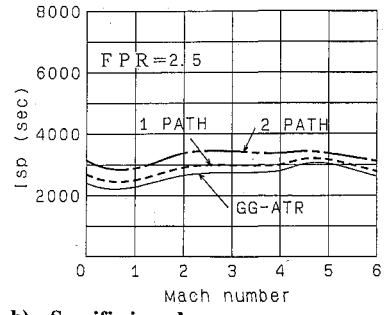

b) Specific impulse

Fig. 8 Performance of PE-ATR: design fan pressure ratio is 2.5; temperature at outlet of heat exchanger is about 500 K in 1-path type and is about 900 K in 2-path type.

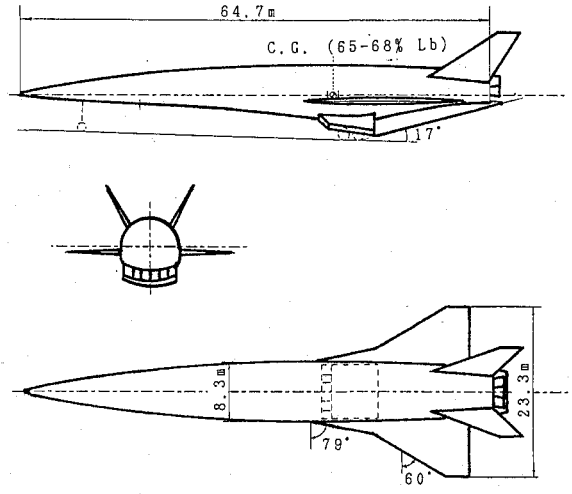

Fig. 9 Configuration of SSTO vehicle.

tributes to the weight reduction of the engine, and so high TIT (2000°C level) and low CPR (about 4.5–6.0) is considered to be one of the best configurations for the TJ engine, as far as the present analysis shows. This will be investigated for the SSTO mission in the next section.

The "basic type" ATR engines, i.e., GG- and Exp-ATR, are shown in Figs. 6 and 7. The design fan pressure ratios (FPR) adopted here are 1.7, 2.5, and 3.5. As mentioned earlier, the *Isp* of the GG-ATR is lower than that of the Exp-ATR because it needs an oxidizer to burn the fuel before the turbine. However, at high flight speeds, GG-ATRs have higher thrust than Exp-ATRs for the same FPR. In the range of high Mach number, lower FPR gives higher *Isp* and higher thrust.

Figures 8 show the performance of a typical PE-ATR (FPR = 2.5), which is illustrated by the comparison with the GG-ATR of the same design FPR. In this study, two kinds of fuel paths in the outer heat exchanger are assumed. In one type, coolant (fuel hydrogen) flows into the nozzle end and fluxes from the outer wall of the combustor as it is heated by the hot

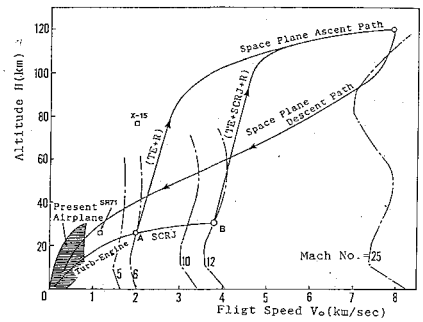

Fig. 10 Flight trajectory for SSTO.

Table 1 Conditions for the single-stage-to-orbit flight analysis

Takeoff gross weight	350 ton
Takeoff wing loading	0.6 ton/m^2
Maximum dynamic pressure	80 kPa
Maximum radiation equilibrium temperature	2000°C
Maximum acceleration	3.5 *g*
Propulsion system	Turboengine × 6 + scram + rocket
Weight of scram engine	0.25 ton/inlet area
T/W of rocket engine	75
Isp of rocket engine	450 s

gas in the combustor and the nozzle. In the other type, coolant moves from the combustor wall to the nozzle end and comes back to the combustor wall then flows into the gas generator. These are called 1-path and 2-path part-expander ATR, for convenience. In the former, the temperature of the coolant at the outlet of the heat exchanger is about 500 K, and in the latter it is about 900 K because of the longer coolant path. Returning to Figs. 8, though the difference between PE- and GG-ATR cannot be seen in thrust, *Isp* of the former is better than that of the latter by about 22%. This is because the temperature of the fuel supplied to the gas generator is increased by the outer heat exchanger in the case of PE-ATR, and so the oxidizer that is necessary to burn the fuel is less than the basic GG-ATR. One of the key technologies of the PE-ATR is to realize such a highly efficient heat exchanger.

IV. Ascent Performance Analysis for SSTO Vehicles

A. Assumptions for Analysis

Our former study[2] clarified the dependence of the remaining weight on the orbit upon the performance (mean thrust weight ratio and mean *Isp* along the flight path) of some kinds of turboengines. This section extends these results, adding the pure-TJ and PE-ATR as the candidates for the propulsion system.

The configuration of the SSTO vehicle used in this flight analysis is shown in Fig. 9. The aerodynamic parameters, such as the lift and drag coefficient, were obtained from the computational fluid dynamics (CFD) analysis and wind-tunnel tests. Wing loading is assumed to be 0.6 ton/m^2 considering the restriction of practical takeoff speed (about Mach 0.5) and length of runway (about 3000 m).

Figure 10 shows the two-dimensional ascent trajectory for the SSTO vehicle on which the dynamic pressure and the limit of radiation equilibrium skin temperature are selected as 80 kPa and 2000°C by imaging practical body structure and advanced surface insulation materials. Maximum acceleration allowed in the flight is assumed to be 3.5 *g*. Ascent schedule after being switched from air-breathing engines to rocket engines is determined to minimize drag and maneuvering loss. The conditions for the SSTO flight analysis are summarized in Table 1.

The performance of the scramjet engines used in the flight analysis of the SSTO vehicle is shown in Figs. 11. These are obtained from the advanced combustion technique, i.e., the

Table 2 Applied materials for the turbojet and ramjet engines

Component	Material	
	TIT ≤1500°C	TIT = 2000°C
Compressor		
Rotor	MMC[a]	AMMC[b]
Stator	MMC[a]	AMMC[b]
Frame	MMC[a]	AMMC[b]
Combustor		
Liner/casing	Nickel base alloy	Ceramics
Turbine		
Rotor	Ceramics	ACC[c]
Stator	Ceramics	ACC[c]
Nozzle	Ceramics	ACC[c]
Frame	MMC[a]	AMMC[b]
After burner/ram burner		
Inner wall	ACC[c] carbon felt	ACC[c] carbon felt
Structure	Nickel base honeycomb	Nickel base honeycomb
Flameholder	Cobalt base alloy	Cobalt base alloy
Nozzle		
Inner wall	ACC[c] carbon felt	ACC[c] carbon felt
Structure	Nickel base honeycomb	Nickel base honeycomb

[a]Metal matrix composite. [b]Advanced metal matrix. [c]Advanced carbon-carbon.

Table 3 Applied materials for the air-turboramjet engines

Component	Material
Fan	
Rotor	AMMC[a]
Stator	FRM
Frame	
Duct	
Turbine	
Rotor	ACC[b]
Stator	ACC[b]
Nozzle	
Frame	
Combustor	
Inner wall	ACC[b] carbon felt
Structure	Nickel base honeycomb
Flameholder	Cobalt base alloy
Nozzle + heat exchanger	
Inner wall	ACC[b] carbon felt
Structure	Nickel base honeycomb AMMC[a]

[a]Advanced metal matrix. [b]Advanced carbon-carbon.

oblique detonation wave combustion,[6] which gives a higher thrust and *Isp* than the state-of-the-art value, as shown in the previous study. The weight of the scramjet engine is assumed to be 0.25 ton per unit inlet cross section, which is based on the advanced material technology. The thrust size of scram engines is determined to minimize the difference between the remaining weight and the scram weight. Total thrust of the rocket engines is selected to be able to get sufficient acceleration. Specific impulse and thrust-to-weight ratio of rocket engines are assumed to be 450 s and 75, respectively. These values are almost equal to those of the Space Shuttle main engine (SSME).

Switching velocities from turbo mode to scram mode and from scram mode to rocket mode influences the mission capability significantly. The former is varied from Mach 5 to 6 in accordance with the maximum operating Mach number of each turboengine. The latter is varied from Mach 7 to 20 in accordance with thrust size and performance of scram engines.

The estimation of each engine weight is based on the considerable advanced material technology level, as shown in Tables 2 and 3. The materials that have high heat resistance, such as advanced metal matrix composite (AMMC), ceramics, and carbon-carbon, are assumed to be applied for the primary parts of the propulsion system.

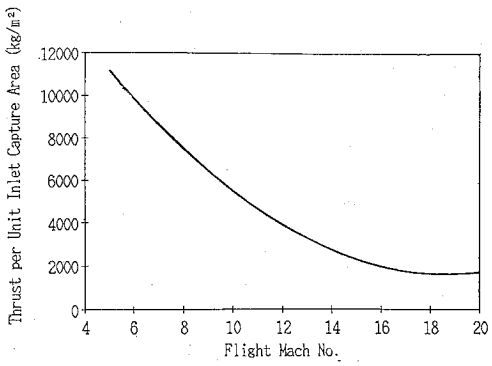

a) Thrust

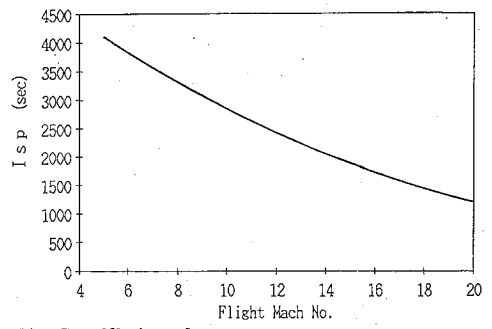

b) Specific impulse

Fig. 11 Performance of scramjet engine used for SSTO flight analysis.

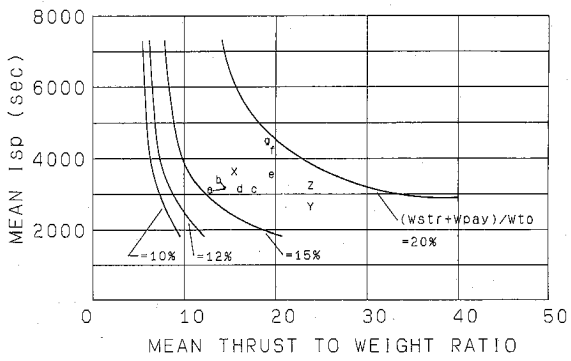

Fig. 12 Ratio of structural and payload weight on the final orbit to takeoff gross weight obtained by various turboengines in SSTO mission—a: TRJ (TIT = 1250°C, CPR = 4.5), over/under type; b: TJR (TIT = 1500°C, CPR = 4.5), over/under type; c: TJR (TIT = 1250°C, CPR = 4.5), tandem type; d: TJ (TIT = 1250°C, CPR = 4.5) with afterburner; e: TJ (TIT = 2000°C, CPR = 4.5) with afterburner; f: dry TJ (TIT = 2000°C, CPR = 4.5); g: dry TJ (TIT = 2000°C, CPR = 6.0); x: Exp-ATR (FPR = 2.5); y: GG-ATR (FPR = 2.5); z: PE-ATR (FPR = 2.5).

B. Results and Considerations

Under the previous assumptions, the remaining weight on the orbit can be described as a function of the mean thrust and *Isp* of the turboengine approximately, as shown in the previous study,[2] i.e.,

$$W_{orb} = W_{orb}(T, Isp) = W_{orb}(T^*, Isp^*)$$

Strictly speaking, the remaining weight depends on the thrust schedule along the specific flight path, but the earlier approximation approach can be useful at the "feasibility study" level. In this paper, only the final result is shown, i.e., the relation between this mean performance and the mission capability (remaining weight ratio on the final orbit) of the turboengine. The details of the process to obtain them are described in the previous paper.

Figure 12 shows the influence of the ratio of the remaining weight, i.e., $(W_{str} + W_{pay})/W_{to}$, on the engine performance,

which is measured by the mean thrust-weight ratio and the mean specific impulse.

The points marked with a and b indicate the over/under TRJ, which show lower mission capability than basic ATRs (namely GG- and Exp-ATR) marked with x and y, which are investigated in the previous study. This is mainly due to the heavy weights of their engines.

The tandem TRJ marked with c has almost the same remaining weight ratio as those of basic ATR engines, about 17%, because the reheat combustion system and the exhaust nozzle are common with TJ and RJ in the tandem configuration so that the engine weight is reduced.

The thrust-to-weight ratio of TJ with afterburning is less than that of tandem TRJ, as illustrated with mark d. This is due to the assumption that the heavier material, such as AMMC, is applied to the compressor rotor since the conventional metals cannot stand the high temperature caused by high flight speed above Mach 4. If the lighter material, such as carbon-carbon, could be used for this section, the engine weight would be reduced and the thrust-to-weight ratio would be improved.

The dry TJ (i.e., TJ with no afterburner) with TIT = 2000°C (marked with f and g) have the best mission capability of all turboengines examined here because no afterburning causes both the high *Isp* and the weight reduction. In the range of this study, it can be said that the dry TJ with high TIT is the best propulsion system, but it must be noted that it is based on the further advanced technology, namely, such high TIT may not be achieved in the near future. However, the material technology is progressing rapidly, so that it may be possible sooner than we expected.

On the other hand, *Isp* of PE-ATR (2 path) is improved compared with GG-ATR, which is almost the same value as those of TRJ engines, as shown with mark z. As explained earlier, this is because fuel heated by the outer heat exchanger around the exhaust system considerably reduces the oxidizer that is necessary to burn the fuel. The remaining weight ratio becomes 18–19% in the case of PE-ATR.

V. Ascent Performance Analysis for the TSTO Vehicle

The objective of this section is to clarify the feasibility of the TSTO vehicle compared with the SSTO vehicle investigated in the previous section.

A. Assumptions

The design data for the TSTO mission analysis are shown in Table 4. The vehicle characteristics (takeoff gross weight, wing loading, and aerodynamic force coefficient, etc.), the limitation for flight trajectory (maximum dynamic pressure and acceleration), and the rocket engine performance are assumed to be the same as in the case of the SSTO analysis. The gross weight of the second stage is varied from 50 to 300 ton and the staging Mach number is from 4.5 to 6.5 in order to examine their influence on the mission capability.

The flight trajectory in the ATR engine mode, i.e., from takeoff to staging speed, is optimized so that the specific excess power per unit fuel consumption, i.e.,

$$\frac{V(F-D)/m}{F/Isp}$$

is minimized until the dynamic pressure on the flight trajectory reaches its maximum value (80 kPa). The flight trajectory is assumed to be in the two-dimensional plane. The pull-up maneuvering is conducted just before staging in order to reduce the maneuvering loss of the second stage.

B. Results and Considerations

The ratio of the effective remaining weight (W_{ef2}: structural weight plus payload weight of the second stage) to the second stage gross weight (W_{gr2}) is the important value because the mission capability is dependent on it. Namely, if it is increased, the requirement of vehicle weight reduction may be moderated and/or the payload weight ratio may be increased. This ratio was also used in the SSTO mission analysis, as shown in Fig. 12.

Figure 13 shows the influence of the second stage gross weight (i.e., the second stage weight at staging point) on W_{ef2}/W_{gr2}. This figure shows that W_{ef2}/W_{gr2} increases as the second stage gross weight increases, but the inclination becomes smaller. At W_{gr2} = 200 ton, W_{ef2}/W_{gr2} is about 20%, which is larger than any in Fig. 12, except those obtained by dry turbojet with TIT = 2000°C. It must be noted that the propulsion system adopted in this TSTO flight analysis needs less advanced technology than the SSTO analysis. For one, no scramjet is equipped in the TSTO mission. Moreover, the scramjet engine used in the previous SSTO analysis is based on the high technology level, such as the detonation wave combustion and the light weight structure (0.25 ton per unit inlet area). If no scramjet is used, i.e., the propulsion system consists of only a turboengine and rocket engine, in SSTO mission, W_{ef}/W_{gr} becomes about 12%, which is equal to 62% of that obtained by the TSTO mission analysis. From this result, it can be said that the TSTO vehicle is more realistic than the

Table 4 Conditions for two-stage-to-orbit flight analysis

Takeoff gross weight	500 ton
Second stage gross weight	50–350 ton
Takeoff wing loading	0.6 ton/m^2
Maximum dynamic pressure	80 kPa
Maximum acceleration	3.5 *g*
First stage powerplant	GG-ATR engine × 6
Second stage powerplant	Rocket engine
T/W of rocket engine	75
Isp of rocket engine	450 s
Staging Mach number	4.5–6.5

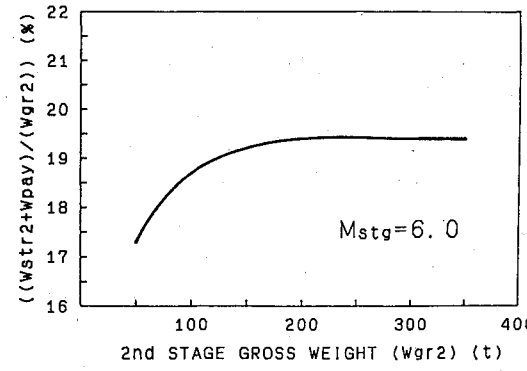

Fig. 13 Influence of the second stage gross weight on (W_{str2} + W_{pay})/W_{gr2}.

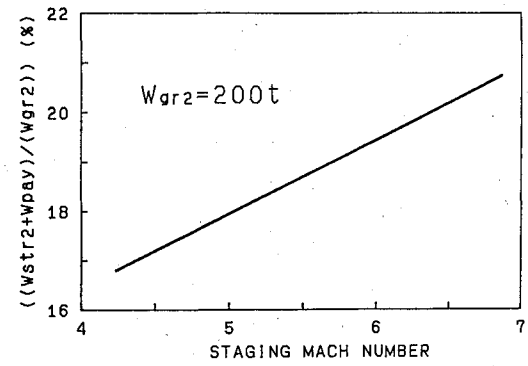

Fig. 14 Influence of the staging Mach number on (W_{str2} + W_{pay})/W_{gr2}.

SSTO vehicle. (It is noted that the flight trajectory and the pull-up maneuvering are not optimized completely in the present study. Therefore, the earlier value, $W_{ef2}/W_{gr2} = 19.5\%$, may be improved by a more detailed procedure to optimize the flight path and the vehicle characteristics.) Figure 14 shows the influence of the staging Mach number on the TSTO mission capability. W_{ef2}/W_{gr2} increases as the staging Mach number increases. It is clear that one of the most important requirements to the turboengine that propels the first stage is to be able to operate at as high a flight speed as possible.

VI. Conclusions

The engine performance, the SSTO mission capability for some kinds of promising turboengines, such as dry TJ, TJ with afterburner, TRJ, GG-, Exp-, and PE-ATR, and the TSTO mission capability were studied. From these results, the following are clarified:

1) The dry TJ with TIT = 2000°C is one of the desirable candidates for the propulsion system of the SSTO vehicle because of its lighter weight and higher *Isp*. However, it depends on the advancement in the field of material technology, which enables such high turbine inlet temperature.

2) The part-expander cycle ATR can improve *Isp* as compared with gas generator cycle ATR because the fuel heated by the outer heat exchanger needs less oxidizer in the precombustion stage. However, such an efficient heat exchanger, which heats up fuel over about 900 K, also needs the advanced design and material technology.

3) Even using the higher performance engines and advanced light materials, the effective remaining weight on the final orbit of the SSTO vehicle cannot exceed 20% of its takeoff gross weight. Namely, in order to achieve the SSTO mission, engine performance, vehicle performance, material technology, etc., must be improved further from the present level.

4) On the other hand, the effective remaining weight obtained in the TSTO mission analysis can reach about 20% of the second stage gross weight with the lower technology level, i.e., without scramjet engine. This result quantitatively shows that the TSTO vehicle is more feasible than the SSTO vehicle apart from the problem of the complexity in the vehicle control.

References

[1]Sakata, K., Minoda, M., Yanagi, R., and Nouse, H., "Conceptual Study on Hypersonic Air-Breathing Engine for Earth to Orbit Vehicle with Turbomachinery Base Technology," AIAA Paper 88-2947, July 1988.

[2]Nouse, H., Minoda, M., Yanagi, R., Tamaki, T., and Fujimura, T., "Conceptual Study of Turbo-Engines for Horizontal Take-off and Landing Space Plane," International Astronautical Federation, Paper 88-253, Oct. 1988.

[3]Tanatsugu, N., Inatani, Y., Makino, T., and Hiroki, T., "Analytical Study of Space Plane Powered by Air-Turbo Ramjet with Intake Air Cooler," International Astronautical Federation, Paper 87-264, Oct. 1987.

[4]Shottle, U. M., Grallert, H., and Hewitt, F. A., "Advanced Air-Breathing Concepts for Winged Launch Vehicles," International Astronautical Federation, Paper 88-248, Oct. 1988.

[5]Koelle, D. E., and Kuczera, H., "SAENGER: Space Transportation System Status Report 1988," International Astronautical Federation, Paper 88-192, Oct. 1988.

[6]Ostrander, M. J., "Standing Oblique Detonation Wave Engine Performance," AIAA Paper 87-2002, May 1987.